Bioorganic & Medicinal Chemistry Letters 20 (2010) 618–622

Contents lists available at ScienceDirect

Bioorganic & Medicinal Chemistry Letters

journal homepage: www.elsevier.com/locate/bmcl

Structure and property based design of factor Xa inhibitors: pyrrolidin-2-ones with monoaryl P4 motifs

Savvas Kleanthous [a], Alan D. Borthwick [a], David Brown [a], Cynthia L. Burns-Kurtis [b], Matthew Campbell [a], Laiq Chaudry [a], Chuen Chan [a], Marie-Olive Clarte [a], Máire A. Convery [a], John D. Harling [a], Eric Hortense [a], Wendy R. Irving [a], Stephanie Irvine [a], Anthony J. Pateman [a], Angela N. Patikis [a], Ivan L. Pinto [a], Derek R. Pollard [a], Theresa J. Roethka [b], Stefan Senger [a], Gita P. Shah [a], Gary J. Stelman [b], John R. Toomey [b], Nigel S. Watson [a], Robert I. West [a], Caroline Whittaker [a], Ping Zhou [a], Robert J. Young [a,*]

[a] GlaxoSmithKline, Medicines Research Centre, Gunnels Wood Road, Stevenage, Hertfordshire SG1 2NY, United Kingdom
[b] GlaxoSmithKline, 709 Swedeland Road, King of Prussia, PA 19406, USA

ARTICLE INFO

Article history:
Received 18 September 2009
Revised 16 November 2009
Accepted 17 November 2009
Available online 20 November 2009

Keywords:
Factor Xa
Oral inhibitors
Property based design
Structure based design
P450 inhibition

ABSTRACT

Structure and property based drug design was exploited in the synthesis of sulfonamidopyrrolidin-2-one-based factor Xa inhibitors, incorporating neutral and basic monoaryl P4 groups, ultimately producing potent inhibitors with effective levels of anticoagulant activity and extended oral pharmacokinetic profiles. However, time dependant inhibition of Cytochrome P450 3A4 was a particular issue with this series.

The selective inhibition of proteases in the blood coagulation cascade has been extensively researched in the pursuit of new small-molecule anticoagulant therapies.[1] This approach offers the prospect of improved efficacy in suppressing thrombosis, whilst reducing the bleeding liability associated with other therapies, thus eliminating the need for intensive monitoring. Recent approvals for selective oral therapies have been achieved with the thrombin inhibitor dabigatran[2] and the factor Xa (fXa) inhibitor rivaroxaban,[3] whilst other molecules have progressed to clinical studies.[4]

Our programme of work on fXa inhibitors has focussed on the sulfonamidopyrrolidin-2-one template, exemplified by our first clinical candidate **1**,[5] featuring the morpholine alanyl amide P4 ligand. We successfully exploited structure based design to explore alternative ligands within this pocket as the basis of our back-up programme, which produced many molecules with attractive levels of potency, but at the cost of sub-optimal overall profiles. Notably, the biaryl derivatives **2** and **3** displayed encouraging pharmacokinetic (PK) exposure,[6] but their excellent potency translated into relatively modest anticoagulant activity (Table 1).

Compounds made to this point were designed within strict hydrophobicity limits ($c\log D_{7.4}$ <4)[9], which often showed tangible benefits in terms of better translation of activity into anticoagulant activity and improved pharmacokinetics. Furthermore, a review of PK data alongside structural properties indicated that a reduction in molecular size was a potential means of improving exposure. ***In this communication, these property based design principles are highlighted in the discovery of a new series of inhibitors.

Inspection of the X-ray crystal structure of **2** bound into fXa suggested that its distal ring could be truncated to either an isopropenyl or carboxamide group, whilst maintaining hydrophobic contacts with the aromatic resides Tyr99, Trp215 and Phe174 in the S4 pocket (Fig. 1). This assessment provided impetus to investigate a novel series of compounds that offered opportunities, through loss of an aromatic ring,[10] to significantly reduce size and maintain or lower hydrophobicity levels.

Synthetic entry into these compounds was established through *tert*-butyl (3*S*)-1-(2-fluoro-4-iodophenyl)-2-oxopyrrolidin-3-yl carbamate **4**, akin to the 4-bromo derivative described in the biaryl series[6a] (Scheme 1). The 2-propenyl substituted

* Corresponding author. Tel.: +44 1438 768372.
E-mail address: Rob.J.Young@gsk.com (R.J. Young).

0960-894X/$ - see front matter © 2009 Elsevier Ltd. All rights reserved.
doi:10.1016/j.bmcl.2009.11.077

Table 1
fXa inhibitory activities,[7] anticoagulant potency[8] and physical descriptors[9] for compounds **1–3**

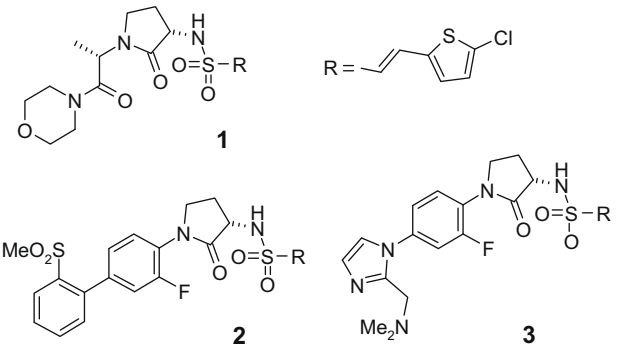

Entry	fXa K_i (nM)	1.5 × PT (μM)	$c\log D_{7.4}$	MW	cmr
1	4	1.2	2.1	447	10.9
2	0.2	21.3	3.0	555	13.7
3	0.2	4.2	2.7	524	13.3

intermediate **5** was prepared via the palladium mediated coupling of **4** with the organozinc reagent generated in situ from 2-bromo-1-propene. Modified Heck coupling of **4** with butyl vinyl ether followed by acid hydrolysis of the derived (1:1) mixture of α and β substituted vinyl ethers afforded methylketone **6**. Primary **7a**, secondary **7b**, and tertiary **7c** amide intermediates were prepared via palladium mediated carbonylation of **4** followed by trapping with the ammonia, methylamine or dimethylamine, respectively. Each intermediate was deprotected under acidic conditions furnishing amines that were derivatised as the (*E*)-2-(5-chloro-2-thienyl)ethenesulfonamides to yield target compounds **8–12**.

Gratifyingly, this set of compounds displayed low nM levels of fXa inhibition[7] and, for the more hydrophilic examples, encouraging levels of anticoagulation[8] (expressed as 1.5 × PT, Table 2); with amide **10** being of similar size (expressed as calculated molar refractivity = 10.7),[9] molecular weight (444) and hydrophobicity ($c\log D_{7.4}$ 2.3) to our first clinical candidate **1** (Table 1).

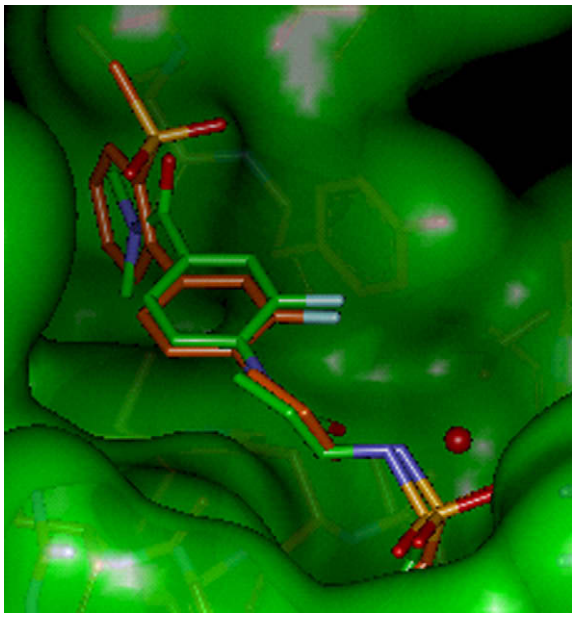

Figure 1. Overlay of a proposed carboxamide onto the X-ray crystal structure of **2** bound into fXa (PDB code 2vh6)[6a], showing the contacts in the S4 pocket.

To capitalise on these findings, our previously successful tactic of improving physical properties by introducing a weakly basic centre into the motif binding in the S4 pocket was explored.[6b,11] This was best achieved, whilst maintaining a similar size and topology, by formal replacement of the carbonyl oxygen of **10** by an alkyl group, thereby generating an α-methyl benzylamine.

Racemic and chiral approaches were exploited in the synthesis of the target compounds. Thus acetophenone **13** was converted into the racemic aminoethyl anilines **14** by reductive amination followed by acidic deprotection of the Boc-protecting group (Scheme 2). Chiral analogues were accessed by reduction of the imine derived from $TiCl_4$ mediated condensation of **13** with either (*S*)- or (*R*)-1-phenylethylamine[12] to give **15** or its enantiomer; this proceeded with high diastereoselectivity.[13] Subsequently, Eschweiler–Clarke methylation, hydrogenolysis of the chiral auxiliary and Boc removal/selective re-introduction were performed in an appropriate order to furnish anilines **16** or **17** of high enantiopurity for further manipulation (Scheme 2).

Protected amino pyrrolidin-2-ones **18** were constructed (Scheme 3) using homoserine lactone/trimethyl aluminium methodology[14] when an unprotected benzylamine was present; alternatively, the orthogonally protected intermediates **19** were accessed from *N*-Cbz-methionine.[15] These were converted into the target compounds **20–35** using the established sequences with appropriate manipulation of Cbz and Boc-protecting groups around the sulfonylation step.

The high potency generated in this series is first illustrated in Table 3 for the *N*,*N*-dimethylamino analogues, with the (*E*)-2-(5-chlorothien-2-yl)ethenyl P1 motif. The initial compound **20**, as a mixture of two diastereomers, showed both excellent inhibition of fXa and good anticoagulant activity; furthermore, the individual diastereomers (**21** and **22**) showed closely similar profiles.

With this basic P4 moiety, the slightly bulkier 6-chloronaphthyl P1 group was also accommodated (**25** and **26**), whilst maintaining good overall physical properties. Although resulting in slightly reduced anticoagulant activity, this modification had beneficial effects on PK profiles, with **25** and **26** displaying low clearances and increased volumes of distribution that contributed to improved half-lives. A range of alkyl substituents on the pendant amine group was investigated (**27–33**, Table 4), but none of the derived analogues showed improved in vitro potency when compared with the *N*,*N*-dimethyl analogues. However, it is noteworthy that better translation of enzyme inhibitory activity into anticoagulant activity was seen across the series when compared with that observed in the biaryl series exemplified by **2** and **3**.

In vitro metabolism studies indicated rapid removal of one methyl group from the *N*,*N*-dimethyl analogues **25** and **26**, giving the *N*-monomethyl analogues **34** and **35**, which were independently synthesised and evaluated (Table 5). Whilst these compounds showed appreciably poorer anticoagulant activities than **25** and **26**, the significantly extended half–lives were indicative of less-frequent dosing regimes. However, the progression of this series was halted due to strong time dependant inhibition of Cyp3A4,[17] which was attributed to the benzylic amine sub-structure, as it was independent of the P1 substituent. Extensive metabolism of a benzylamine group was noted in DPC423,[18] another fXa inhibitor, which gave rise to reactive intermediates that could cause irreversible damage of the Cyp structure.[19]

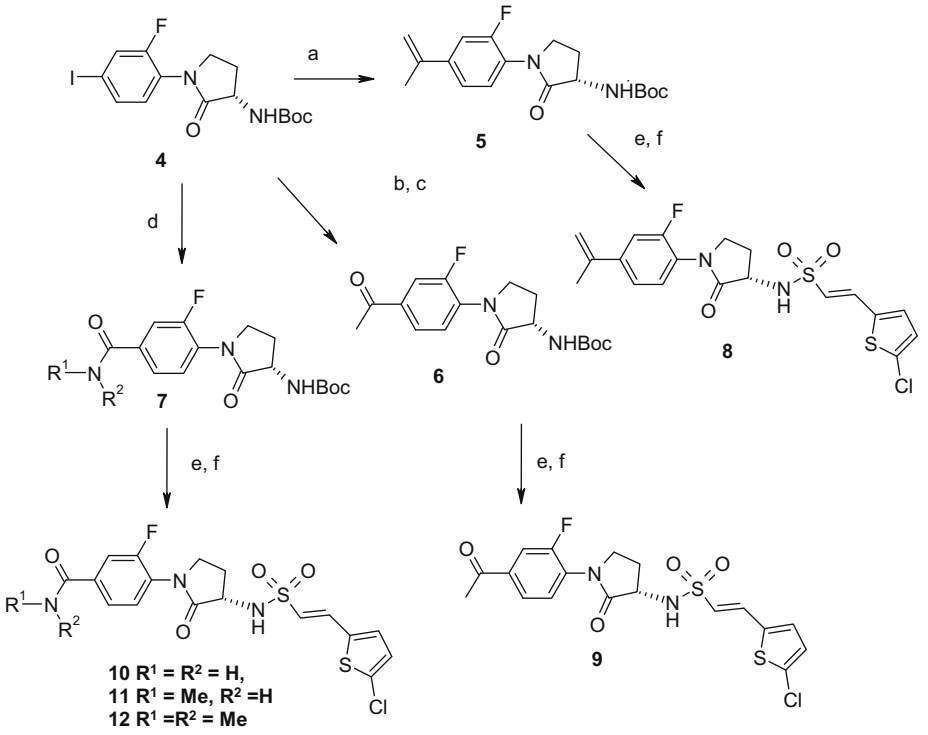

Scheme 1. Reagents and conditions: (a) *n*BuLi, MeC(Br)CH_2, THF, −78 °C; then $ZnCl_2$, Et_2O; $PdCl_2(PPh_3)_2$, THF, −78–20 °C; (b) butyl vinyl ether, Na_2CO_3, Et_3N, $Pd(OAc)_2$, DPPP, DMF, 80 °C; (c) 0.1% HCO_2H, H_2O, MeCN, rt; (d) CO (gas), $PdCl_2(PPh_3)_2$ DMF, NH_3, $MeNH_2$ or Me_2NH, 80 °C; (e) 4 M HCl/Dioxane, rt; (f) RSO_2Cl, DIPEA, MeCN, rt.

Table 2
fXa inhibitory activities[7] anticoagulant potency[8] and physical descriptors[9] for compounds **8–12**

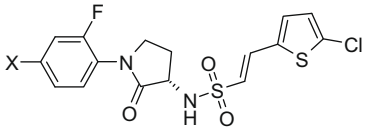

Entry	X	fXa K_i (nM)	1.5 × PT (μM)	*c* log $D_{7.4}$	cmr	MW
8	$C(CH_2)CH_3$	6.2	>100	3.9	11.2	441
9	$C(O)CH_3$	6.0	>100	3.2	10.8	443
10	$C(O)NH_2$	5.1	7.7	2.3	10.7	444
11	C(O)NHMe	35	19.6	2.3	11.1	458
12	$C(O)NMe_2$	1.5	6.5	2.0	11.6	472

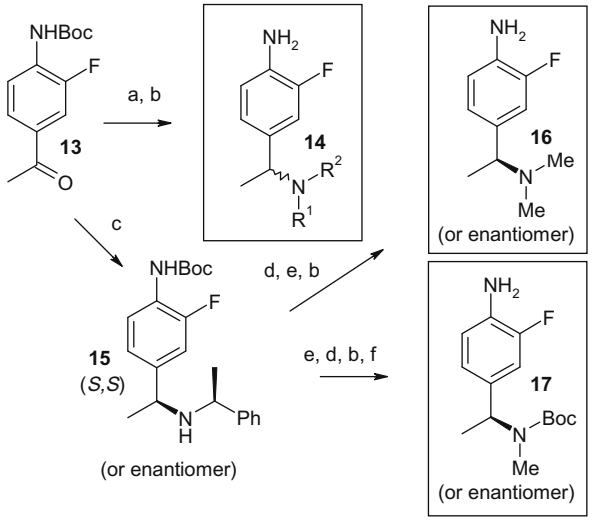

Scheme 2. Reagents and conditions: (a) R^1R^2NH, $NaHB(OAc)_3$, AcOH, THF, rt; (b) HCl, dioxane, rt; or HCl, MeOH, rt; (c) $PhCH(Me)NH_2$, Et_3N, $TiCl_4$, PhMe, −78 °C; then $NaBH_4$, MeOH −78 °C; (d) H_2, 50 psi, $Pd(OH)_2$–C, EtOH 60 °C; (e) $H_2C{=}O$, HCO_2H, MeOH, Δ; (f) Boc_2O, DCM, rt.

Although the benzylic amine motif in this series and that in DPC423 are closely similar, this is not reflected in their fXa binding modes. The 3-aminomethylphenyl group in DPC423 binds in the P1 pocket[20] whereas X-ray structures[21] of **21** and **22** bound into fXa (Fig. 2) clearly showed the related sub-unit in the P4 pocket where the diastereomeric methyl groups make hydrophobic contacts with the Trp215 residue and the amino group nitrogen is within hydrogen bonding distance of the backbone carbonyl of Glu97. The S1 pocket is occupied by the aromatic sulfonamide group as seen throughout previously reported series.[5,6,11]

In conclusion: the compounds described in this paper further explored chemical space, defined by size and hydrophobicity, similar to our first clinical candidate, resulting in effective anticoagulant activity with enhanced oral pharmacokinetic half–lives. However, further profiling of the molecules indicated time dependant inhibition of Cyp3A4. Important lessons learned with these compounds were subsequently exploited in potent, long-acting molecules without P450 liabilities, which will be reported in future communications.

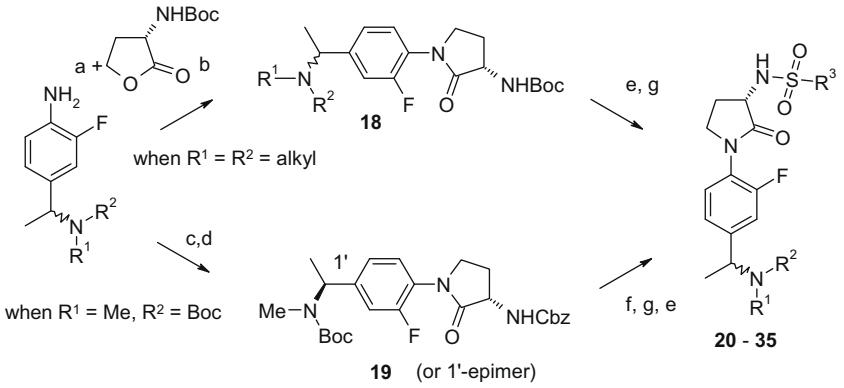

Scheme 3. Reagents and conditions: (a) Me_3Al, DCM, 0 °C to rt; (b) DtBAD, Bu_3P, THF, rt; (c) CbzMetOH, HATU, DIPEA, DCM, rt; (d) MeI, MeCN, 60 °C, then Cs_2CO_3; (e) HCl, MeOH, rt; (f) H_2, $Pd(OH)_2$–C, EtOH, rt; (g) R^3SO_2Cl, pyridine, MeCN, rt.

Table 3
fXa inhibitory activities,[7] anticoagulant potency,[8] physical descriptors[9] and PK parameters[16] for compounds **20**–**26**

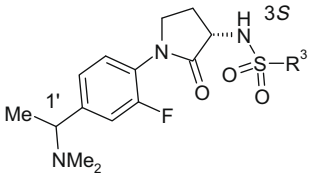

Entry	1′-Stereo	R^3	fXa K_i (nM)	1.5 × PT (μM)	MW	*c* log $D_{7.4}$	cmr	Clp[a] (ml/min/kg)	$T_{1/2}$[b] (h)	Vss[c] (L/kg)	F[d] (%)
20	*R*/*S*	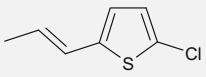	0.8	0.9	472	2.2	12.0	—	—	—	—
21	*R*		2	0.7				7.5	1.3	0.66	54
22	*S*		1	0.9				4.3	1.6	0.53	23
23	*R*/*S*	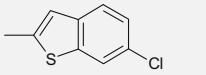	5	3.8	496	2.4	12.8	2.1	3.1	0.52	10
24	*R*/*S*	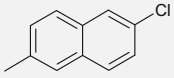	0.8	2.9	490	2.4	12.9	-	—	—	—
25	*R*		2	1.9				8	2.6	1.3	43
26	*S*		2	2.1				13	2.1	1.8	81

[a] Clp, plasma clearance expressed as mL/min/kg.
[b] $T_{1/2}$, half-life of the test compound expressed in hours.
[c] Vss, steady state volume of distribution expressed as L/kg.
[d] *F*, oral bioavailability expressed as percentage.

Table 4
fXa inhibitory activities[7] and anticoagulant potency[8] for compounds **27**–**33**

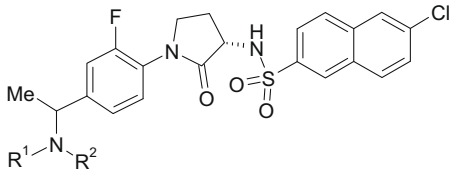

Entry	NR^1R^2	fXa K_i (nM)	1.5 × PT (μM)
24	NMe_2	0.8	2.9
27	NEtMe	6	4.4
28	NHEt	3	11.2
29	NH-*i*-Pr	20	23.6
30	NMe-*i*-Pr	9	6
31	Azetidinyl	4	5.3
32	Pyrrolidinyl	4	4.1
33	Piperidinyl	2	5.5

Table 5
fXa inhibitory activities,[7] anticoagulant potency,[8] physical descriptors[9] and PK parameters[16] for compounds **34** and **35**

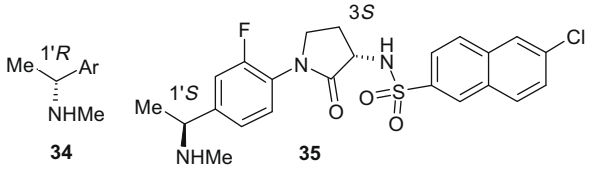

Entry	1′-Stereo	fXa K_i (nM)	1.5 × PT (μM)	MW	*c* log $D_{7.4}$	cmr	Clp[a] (ml/min/kg)	$T_{1/2}$[b] (h)	Vss[c] (L/kg)	F[d] (%)
34	*R*	4	6.9	476	1.6	12.5	1.6	18	2.4	>10[A]
35	*S*	2	7.0	476	1.6	12.5	3.1	15	3.3	>15[A]

[a,b,c,d] as Table 3.
[A] These *F*% data are low estimates of the true figure due to the extended half-lives.

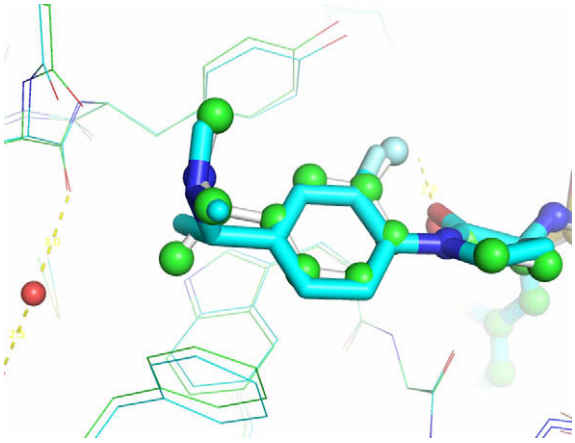

Figure 2. X-ray crystal structures of the compounds **21** and **22** bound into fXa, highlighting S4 interactions as described in the text.

References and notes

1. (a) Gustafsson, D.; Bylund, R.; Antonsson, T.; Nilsson, I.; Nystroem, J.-E.; Eriksson, U.; Bredberg, U.; Teger-Nilsson, A.-C. *Nat. Rev. Drug Disc.* **2004**, *3*, 649; (b) Saiah, E.; Soares, C. *Curr. Top. Med. Chem.* **2005**, *5*, 1677.
2. (a) Eikelboom, J. E.; Weitz, J. I. *Thromb. Haemost.* **2009**, *101*, 2; (b) Sanford, M.; Plosker, G. L. *Drugs* **2008**, *68*, 1699; (c) Sobera, L. A.; Bozzo, J.; Castaner, J. *Drugs Future* **2005**, *30*, 877.
3. (a) Abrams, P. J.; Emerson, C. R. *Pharmacotherapy* **2009**, *29*, 167; (b) Escolar, G.; Villalta, J.; Casals, F.; Bozzo, J.; Serradell, N.; Bolos, J. *Drugs Future* **2006**, *31*, 484.
4. (a) Spyropoulos, A. C. *Thromb. Res.* **2008**, *123*, S29; (b) Ma, Q. *Br. J. Clin. Pharmacol.* **2007**, *64*, 263; (c) Eriksson, B. I.; Quinlan, D. J.; Weitz, J. I. *Clin. Pharmacokinet.* **2009**, *48*, 1.
5. (a) Chan, C.; Borthwick, A. D.; Brown, D.; Burns-Kurtis, C. L.; Campbell, M.; Chaudry, L.; Chung, C.-W.; Convery, M. A.; Hamblin, J. N.; Johnstone, L.; Kelly, H. A.; Kleanthous, S.; Patikis, A.; Patel, C.; Pateman, A. J.; Senger, S.; Shah, G. P.; Toomey, J. R.; Watson, N. S.; Weston, H. E.; Whitworth, C.; Young, R. J.; Zhou, P. *J. Med. Chem.* **2007**, *50*, 1546; (b) Abboud, M. A.; Needle, S. J.; Burns-Kurtis, C. L.; Valocik, R. E.; Koster, P. F.; Amour, A. J.; Chan, C.; Brown, D.; Chaudry, L.; Zhou, P.; Patikis, A.; Patel, C.; Pateman, A. J.; Young, R. J.; Watson, N. S.; Toomey, J. R. *J. Cardiovasc. Pharmacol.* **2008**, *52*, 66.
6. (a) Young, R. J.; Borthwick, A. D.; Brown, D.; Burns-Kurtis, C. L.; Campbell, M.; Chan, C.; Charbaut, M.; Chung, C.-w.; Convery, M. A.; Kelly, H. A.; King, N. P.; Kleanthous, S.; Mason, A. M.; Pateman, A. J.; Patikis, A. N.; Pinto, I. L.; Pollard, D. R.; Senger, S.; Shah, G. P.; Toomey, J. R.; Watson, N. S.; Weston, H. E. *Bioorg. Med. Chem. Lett.* **2008**, *18*, 23; (b) Young, R. J.; Borthwick, A. D.; Brown, D.; Burns-Kurtis, C. L.; Campbell, M.; Chan, C.; Charbaut, M.; Convery, M. A.; Diallo, H.; Hortense, E.; Irving, W. R.; Kelly, H. A.; King, N. P.; Kleanthous, S.; Mason, A. M.; Pateman, A. J.; Patikis, A. N.; Pinto, I. L.; Pollard, D. R.; Senger, S.; Shah, G. P.; Toomey, J. R.; Watson, N. S.; Weston, H. E.; Zhou, P. *Bioorg. Med. Chem. Lett.* **2008**, *18*, 28.
7. Factor Xa inhibitory activities were determined using Rhodamine 110, bis-(CBZ-glycylglycyl)-L-arginine amide as the fluorogenic substrate; details are described in Ref. 5a.
8. Anticoagulant activities were determined in the prothrombin time (PT) assay; see Ref. 5a, expressed as the concentration required to extend the control coagulation time by 50% (1.5 × PT).
9. Hydrophobicity predictions, expressed as *c* log $D_{7.4}$, were all re-calculated using Advanced Chemistry Development software v11.0 to ensure consistency in this paper; calculated molecular refractivity (cmr) was derived from Daylight software v4.9.
10. Ritchie, T. J.; MacDonald, S. J. F. *Drug Discovery Today* **2009**, *14*, 1011.
11. Young, R. J.; Campbell, M.; Borthwick, A. D.; Brown, D.; Burns-Kurtis, C. L.; Chan, C.; Convery, M. A.; Crowe, M. C.; Dayal, S.; Diallo, H.; Kelly, H. A.; King, N. P.; Kleanthous, S.; Mason, A. M.; Mordaunt, J. E.; Patel, C.; Pateman, A. J.; Senger, S.; Shah, G. P.; Smith, P. W.; Watson, N. S.; Weston, H. E.; Zhou, P. *Bioorg. Med. Chem. Lett.* **2006**, *16*, 5953.
12. (a) Wu, Y.-J.; He, H.; Sun, L.-Q.; Wu, D.; Gao, Q.; Li, H.-L. *Bioorg. Med. Chem. Lett.* **2003**, *13*, 1725; (b) Nugent, T. C.; Ghosh, A. K.; Wakchaure, V. N.; Mohanty, R. R. *Adv. Synth. Catal.* **2006**, *348*, 1289.
13. The reduction to produce **15** typically proceeded with about 9:1 diastereoselectivity. This diastereomeric ratio was enhanced by normal phase chromatography, typically furnishing product of >90% ee at this centre.
14. Bell, I. M.; Beshore, D. C.; Gallicchio, S. N.; Williams, T. M. *Tetrahedron Lett.* **2000**, *41*, 1141. Typically this reaction furnished products with ee's comparable to those reported in this paper and Ref. 6, as determined by ^{19}F NMR of Mosher amide derivatives of deblocked **18** and/or by chiral hplc analysis of final compounds.
15. See Ref. 5a; ^{19}F NMR of Mosher amides of the intermediate amines formed by hydrogenolysis of **19** suggested these transformations gave homochirality at this centre.
16. Pharmacokinetics measured in male Sprague–Dawley rats following intravenous and oral administration. The formulation used for both iv and po dosing was a 5:95% (v/v) mixture of DMSO and 50:50 PEG-200: sterile water. Serial blood samples were collected into heparinised containers at various time-points and blood centrifuged to yield plasma. These studies used at least three animals for each (iv/po) leg.
17. Time dependant inhibition was determined by comparing the activity of CYP3A4 in bactosomes (Cypex ltd, Dundee, Scotland) when incubated with compound at its IC_{50} for zero and 25 min (10 μM concentration of **34** and 33 μM of **35**). Over 25 min **34** showed a 17-fold decrease in activity of Diethoxyfluorescein (DEF) substrate turnover with Cyp3A4 and **35** an 8.5-fold decrease. Experiments with human liver microsomes gave similar results.
18. (a) Mutlib, A. E.; Shockcor, J.; Chen, S.-Y.; Espina, R. J.; Pinto, D. J.; Orwat, M. J.; Prakash, S. R.; Gan, L.-S. *Chem. Res. Toxicol.* **2002**, *15*, 48; (b) Mutlib, A. E.; Chen, S.-Y.; Espina, R. J.; Shockcor, J.; Prakash, S. R.; Gan, L.-S. *Chem. Res. Toxicol.* **2002**, *15*, 63.
19. (a) Kalgutkar, A. S.; Gardner, I.; Obach, R. S.; Shaffer, C. L.; Callegari, E.; Henne, K. R.; Mutlib, A. E.; Dalvie, D. K.; Lee, J. S.; Nakai, Y.; O'Donnell, J. P.; Boer, J.; Harriman, S. P. *Curr. Drug Metab.* **2005**, *6*, 161; (b) Kalgutkar, A. S.; Obach, R. S.; Maurer, T. S. *Curr. Drug Metab.* **2007**, *8*, 407.
20. Pinto, D. J. P.; Orwat, M. J.; Wang, S.; Fevig, J. M.; Quan, M. L.; Amparo, E.; Cacciola, J.; Rossi, K. A.; Alexander, R. S.; Smallwood, A. M.; Luettgen, J. M.; Liang, L.; Aungst, B. J.; Wright, M. R.; Knabb, R. M.; Wong, P. C.; Wexler, R. R.; Lam, P. Y. S. *J. Med. Chem.* **2001**, *44*, 566.
21. The structure for **21** was refined at 1.9 Å (overall Rmerge is 0.089) in Refmac5 to a final Rfactor of 0.196 and Rfree of 0.234 and **22** was refined at 2.4 Å (overall Rmerge is 0.055) in Refmac5 to a final Rfactor of 0.197 and Rfree of 0.255 using procedures described in Ref. 5a. Coordinates are deposited in the protein data bank with codes 2wyg **21** and 2wyj **22**.